AN IMPROVED TIME DOMAIN FINITE ELEMENT-BOUNDARY INTEGRAL SCHEME FOR ELECTROMAGNETIC SCATTERING FROM 3-D OBJECTS

Z. J. Qiu, J. D. Xu, G. Wei, and X. Y. Hou

School of Electronic and Information
Northwestern Polytechnical University
Xi'an 710072, Shaanxi, China

Abstract—This paper proposes an improved time domain finite element-boundary integral scheme for 3-D scattering from arbitrary-shaped objects. The proposed scheme, which uses only one auxiliary boundary, is more efficient than the one reported in the literature that uses two auxiliary boundaries. While preserving the sparseness and symmetry of the finite element matrices, the proposed scheme reduces the computational domain for the finite elements. A major difficulty, here, is the treatment of the singularity of Green's function arising from this scheme. To overcome this problem, the contribution of singular point is computed analytically, and equivalent transformation technique is also included to reduce the integrals' singularity. And, a remedy is presented for the numerical error encountered in the course of the equivalent transformation, which essentially may be attributed to the inherent routine with the time domain finite element-boundary integral method. The validity and accuracy of the hybrid scheme are verified by numerical tests.

1. INTRODUCTION

Finite element-boundary integral (FE-BI) method is a powerful numerical technique for electromagnetic scattering problems, especially for those involving inhomogeneous objects. The hybrid method remains the advantages both of the finite element method and the boundary integral method, and has been widely used and well developed in frequency domain [1–6].

In recent years, as more interests have been focused on time domain method [7–9], the FE-BI method in time domain also has

received increasing attention [10–12]. In [10, 11], a time domain FE-BI scheme is presented for 2-D scattering, and has also been applied to 3-D scattering problems [12]. In this scheme, two auxiliary boundaries are used, one serving as the truncation boundary, and the other serving as the source boundary. Compared to the FE-BI method in frequency domain, this scheme has advantages that the sparseness and symmetry of the finite element matrices are preserved, and that the singularity of Green's function is circumvented.

However, as is well known, the FE-BI hybrid method is exact, and the truncation boundary may be arbitrarily close to the scatter, which in turn leads to minimal computational domain for the finite elements. But, the FE-BI method in time domain with the scheme that uses two auxiliary boundaries will lead to larger computational domain compared with its frequency domain counterpart. For example, if a conducting scatter is considered by time domain FE-BI method using this scheme, usually a two-layer element has to be set between the truncation boundary and the PEC surface. And if the scattering problem of a dielectric one is considered, as another example, with the frequency domain FE-BI method, we may directly choose the scatter's surface as the truncation boundary. However, for the time domain FE-BI method with the above scheme, we have to employ an artificial surface outside the scatter as the truncation boundary, by which additional computational region is introduced. So, in this sense, it is less efficient compared with its frequency domain counterpart.

This paper proposes to remove the inefficiency with the time domain FE-BI method by using only one auxiliary boundary, which may be viewed as the extension of the familiar frequency domain scheme to the time domain. Compared to the scheme that uses two auxiliary boundaries, while preserving the sparseness and symmetry of finite element matrices, the proposed scheme allows the truncation boundary to take on any shape and to be placed arbitrarily close to the scatter.

However, a major difficulty is with this scheme, i.e., the numerical treatment of the singularity of Green's function. To overcome this problem, we calculate the contribution of singular point analytically. Yet, it is still difficult to calculate some of the integrals accurately as source point close to field point, whose singularity being of higher order. We alleviate the difficulty by applying equivalent transformation technique to these integrals to reduce their singularity. Unfortunately, here, another problem comes up with the equivalent transformation, which essentially may be attributed to the routine of the time domain FE-BI method. To give a remedy for this problem, in contrast to the usual boundary integral method where the equivalent electric and

magnetic currents (i.e., the tangential components of magnetic and electric fields on source boundary) are used, the normal component of the electric field is considered.

The rest of this paper is organized as follows. First, the formulation for the proposed scheme is developed, where a boundary condition similar to the case of combined field integral equation used in frequency domain has been adopted so as to be free of interior resonance. Then, the treatment of the singularity of Green's function with this scheme is addressed. Finally, we demonstrate the validity and accuracy of the proposed scheme by numerical tests, where, for comparison, the scheme that uses two auxiliary boundaries is also considered.

2. FORMULATION

Let us consider a typical problem of EM scattering by an arbitrary-shaped and inhomogeneous object. We introduce an artificial surface S to terminate the computational domain for finite elements, and assume that the region outside S is free space. Inside S, the field $\mathbf{E}$ satisfies

$$\nabla \times [\mu_r^{-1} \nabla \times \mathbf{E}(\mathbf{r}, t)] + \mu_0 \varepsilon \partial_t^2 \mathbf{E}(\mathbf{r}, t) + \sigma \mu_0 \partial_t \mathbf{E}(\mathbf{r}, t) = 0 \qquad \mathbf{r} \in V \tag{1}$$

where V denotes the volume enclosed by S. For a unique solution, it is necessary to impose a boundary condition on S. To be free of interior resonance, we choose a boundary condition similar to the combined field integral equation (CFIE) [13] used in frequency domain

$$\mathbf{n} \times [\mu_r^{-1} \nabla \times \mathbf{E}(\mathbf{r}, t)] + c^{-1} \mathbf{n} \times \partial_t [\mathbf{n} \times \mathbf{E}(\mathbf{r}, t)]|_{S^-}$$
$$= -\mathbf{n} \times \mu_0 \partial_t \mathbf{H}(\mathbf{r}, t) + c^{-1} \mathbf{n} \times \partial_t [\mathbf{n} \times \mathbf{E}(\mathbf{r}, t)]|_{S^+} \tag{2}$$

where $\mathbf{n}$ denotes the outward unit vector normal to S, S^- denotes the surface just interior to S, and S^+ denotes the surface just exterior to S.

The solution to the boundary-value problem defined by equation (1) and (2) can be obtained by seeking the stationary point of the functional

$$
\begin{aligned}
F[\mathbf{E}(\mathbf{r}, t)] = {}& \frac{1}{2} \iiint_V \big\{ \mu_r^{-1} [\nabla \times \mathbf{E}(\mathbf{r}, t)] \cdot [\nabla \times \mathbf{E}(\mathbf{r}, t)] \\
& + \mu_0 \varepsilon \partial_t^2 \mathbf{E}(\mathbf{r}, t) \cdot \mathbf{E}(\mathbf{r}, t) + \sigma \mu_0 \partial_t \mathbf{E}(\mathbf{r}, t) \cdot \mathbf{E}(\mathbf{r}, t) \big\} dV \\
& + \frac{1}{2} \iint_S \big\{ c^{-1} \partial_t [n \times \mathbf{E}(\mathbf{r}, t)] \cdot [\mathbf{n} \times \mathbf{E}(\mathbf{r}, t)] \\
& + 2 \mathbf{E}(\mathbf{r}, t) \cdot \mathbf{V}_s(\mathbf{r}, t) \big\} dS
\end{aligned}
\tag{3}
$$

where $\mathbf{V}_s(\mathbf{r}, t)$ represents the right side of (2). That is,

$$\mathbf{V}_s(\mathbf{r}, t) = -\mathbf{n} \times \mu_0 \partial_t \mathbf{H}(\mathbf{r}, t) + c^{-1}\mathbf{n} \times \partial_t[\mathbf{n} \times \mathbf{E}(\mathbf{r}, t)] \qquad (4)$$

To compute $\mathbf{V}_s(\mathbf{r}, t)$, usually another artificial surface is introduced as the source boundary. However, as pointed out earlier, this would lead to larger computational domain for finite elements, and render the time domain FE-BI method less efficient. So, here, we directly choose the truncation boundary S as the source boundary. The electric and magnetic field in (4) are given as

$$\mathbf{E}(\mathbf{r}, t) = \mathbf{E}^i(\mathbf{r}, t) + \int_{-\infty}^{t} c^2 \nabla\nabla \cdot \mathbf{A}(\mathbf{r}, \tau)d\tau - \partial_t \mathbf{A}(\mathbf{r}, t) - \varepsilon^{-1}\nabla \times \mathbf{F}(\mathbf{r}, t)$$

$$(5)$$

and

$$\mathbf{H}(\mathbf{r}, t) = \mathbf{H}^i(\mathbf{r}, t) + \int_{-\infty}^{t} c^2 \nabla\nabla \cdot \mathbf{F}(\mathbf{r}, \tau)d\tau - \partial_t \mathbf{F}(\mathbf{r}, t) + \mu^{-1}\nabla \times \mathbf{A}(\mathbf{r}, t)$$

$$(6)$$

where

$$\mathbf{A}(\mathbf{r}, t) = \mu_0 \iint_S \mathbf{J}(\mathbf{r}', t) * g(|\mathbf{r} - \mathbf{r}'|, t)dS' \qquad (7)$$

and

$$\mathbf{F}(\mathbf{r}, t) = \varepsilon_0 \iint_S \mathbf{M}(\mathbf{r}', t) * g(|\mathbf{r} - \mathbf{r}'|, t)dS' \qquad (8)$$

In the above equations, "$*$" stands for the convolution, $g(|\mathbf{r} - \mathbf{r}'|, t)$ denotes the 3D free-space Green's function, and $\mathbf{J}$ and $\mathbf{M}$ are the equivalent electric and magnetic currents, defined on surface S, respectively as

$$\mathbf{M}(\mathbf{r}', t) = \mathbf{E}(\mathbf{r}', t) \times \mathbf{n} \qquad \mathbf{r}' \in S \qquad (9)$$

and

$$\mathbf{J}(\mathbf{r}', t) = -\mathbf{n} \times \{\mu^{-1}\partial_t^{-1}[\nabla' \times \mathbf{E}(\mathbf{r}', t)]\} \qquad \mathbf{r}' \in S \qquad (10)$$

The notation ∂_t^{-1} in (10) denotes temporal integration.

3. TREATMENT OF SINGULAR INTEGRALS

We discretize volume V by tetrahedra, and use Whitney 1-form basis functions [14] to approximate the electric field in (3)

$$\mathbf{E}(\mathbf{r},t) = \sum_{i=1}^{N} e_i(t)\mathbf{W}_i(\mathbf{r}) \tag{11}$$

where N denotes the total number of edges, and $\mathbf{W}_i$ denotes Whitney 1-form basis function. According to the finite element's procedure, the space discretization of (3) results in a second-order differential system

$$\mathbf{T}\frac{d^2 e(t)}{dt^2} + (\mathbf{R} + \mathbf{Q})\frac{de(t)}{dt} + \mathbf{S}e(t) + v(t) = 0 \tag{12}$$

The calculation of matrices $\mathbf{T}$, $\mathbf{R}$, $\mathbf{Q}$, and $\mathbf{S}$ is straightforward, and is not presented here.

Now, let us consider the calculation of column vector $v(t)$. Its elements are given by

$$\begin{aligned}
v_i^m(t) = {} & \iint_{S^m} dS\, \mathbf{W}_i^m(\mathbf{r}) \cdot \{c^{-1}\mathbf{n} \times \mathbf{n} \times [\partial_t \mathbf{E}^i(\mathbf{r},t) \\
& + c^2 \nabla\nabla \cdot \mathbf{A}(\mathbf{r},t) - \partial_t^2 \mathbf{A}(\mathbf{r},t) - \varepsilon^{-1}\partial_t \nabla \times \mathbf{F}(\mathbf{r},t)] \\
& - \mu_0 \mathbf{n} \times [\partial_t \mathbf{H}^i(\mathbf{r},t) + c^2 \nabla\nabla \cdot \mathbf{F}(\mathbf{r},t) - \partial_t^2 \mathbf{F}(\mathbf{r},t) \\
& + \mu^{-1}\partial_t \nabla \times \mathbf{A}(\mathbf{r},t)]\}
\end{aligned} \tag{13}$$

By the expressions of magnetic and electric vector potentials $\mathbf{F}$ and $\mathbf{A}$, it is obvious that the integrands in (13) are singular at $\mathbf{r}' = \mathbf{r}$.

First, we consider the following two integrals involved in $v_i^m(t)$

$$I_{h3}^m = \iint_{S^m} \mathbf{W}_i^m(\mathbf{r}) \cdot [\mathbf{n} \times \nabla\nabla \cdot \mathbf{F}(\mathbf{r},t)]\, dS \tag{14}$$

and

$$I_{e3}^m = \iint_{S^m} \mathbf{W}_i^m(\mathbf{r}) \cdot [\mathbf{n} \times \mathbf{n} \times \nabla\nabla \cdot \mathbf{A}(\mathbf{r},t)]\, dS \tag{15}$$

We may note that, there are two "∇" operators acting on the Green's function in (14) and (15). So, the above two integrals have an order $1/R^3$ singularity, and their numerical calculation turns to be impossible. To reduce their singularity, by applying Gauss divergence theorem, we can get

$$\nabla \cdot \mathbf{F}(\mathbf{r},t) = \varepsilon_0 \iint_S \nabla_s' \cdot \mathbf{M}(\mathbf{r}',t) * g(|\mathbf{r} - \mathbf{r}'|,t)\, dS' \tag{16}$$

and

$$\nabla \cdot \mathbf{A}(\mathbf{r},t) = \mu_0 \iint_S \nabla'_s \cdot \mathbf{J}(\mathbf{r}',t) * g(|\mathbf{r} - \mathbf{r}'|,t) dS' \qquad (17)$$

where one of the two "∇" operators has been removed from the Green's function. However, even so, it is still difficult to calculate $v_i^m(t)$ directly by numerical method, for some of the singular integrals with it are of order $1/R^2$.

So, next, we consider evaluating the contribution of singular point analytically before $v_i^m(t)$ is calculated by numerical method. It can be verified that

$$\int_{-\infty}^t c^2 \nabla \nabla \cdot \mathbf{A}(\mathbf{r},\tau) d\tau - \partial_t \mathbf{A}(\mathbf{r},t) - \varepsilon^{-1} \nabla \times \mathbf{F}(\mathbf{r},t)$$

$$= \oiint_S dS' \{ [\mathbf{n} \times \mathbf{E}(\mathbf{r}',t) * \times \nabla' g(|\mathbf{r} - \mathbf{r}'|,t)]$$

$$- \left[\mu \mathbf{n} \times \frac{\partial \mathbf{H}(\mathbf{r}',t)}{\partial t} * g(|\mathbf{r} - \mathbf{r}'|,t) \right]$$

$$+ [\mathbf{E}(\mathbf{r}',t) \cdot \mathbf{n}] * \nabla' g(|\mathbf{r} - \mathbf{r}'|,t) \} \qquad (18)$$

where "$*\times$" stands for the presence of both the convolution and cross operation.

Assume S to be a smooth surface (In FE-BI method, usually a smooth surface is chosen as the truncation boundary). Considering $\mathbf{r}$ closes to S from outer, we separate S into two parts, as shown in Fig. 1, where S_0 denotes the small spherical surface surrounding point $\mathbf{r}$. Now we compute the integral over S_0 as $R = |\mathbf{r} - \mathbf{r}'| \to 0$.
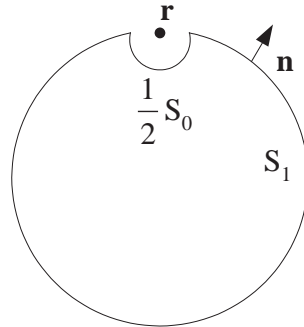

Figure 1. Calculation of singular point's contribution.

With (18), as $R \to 0$, the integral over S_0 may written as

$$I_0 = \oiint_{S_0} dS' \frac{1}{4\pi R^2} \{ \mathbf{n} \times \mathbf{E}(\mathbf{r}', t - R/c) \times \mathbf{e}_R + [\mathbf{n} \cdot \mathbf{E}(\mathbf{r}', t - R/c)] \mathbf{e}_R \} \tag{19}$$

where $\mathbf{e}_R = \frac{\mathbf{r}-\mathbf{r}'}{R}$. On obtaining (19), $1/R$ terms have been omitted, whose contribution to the integral vanishes as $R \to 0$. Note that, on the spherical surface S_0, $\mathbf{n} = \mathbf{e}_R$, with which it can be derived from (19) that $I_0 = \mathbf{E}(\mathbf{r}, t)$.

Therefore, we may write (18) as

$$\int_{-\infty}^{t} c^2 \nabla \nabla \cdot \mathbf{A}(\mathbf{r}, \tau) d\tau - \partial_t \mathbf{A}(\mathbf{r}, t) - \varepsilon^{-1} \nabla \times \mathbf{F}(\mathbf{r}, t)$$

$$= \iint_{S_1} dS' \{ [\mathbf{n} \times \mathbf{E}(\mathbf{r}', t) * \times \nabla' g(|\mathbf{r} - \mathbf{r}'|, t)]$$

$$- \left[\mu \mathbf{n} \times \frac{\partial \mathbf{H}(\mathbf{r}', t)}{\partial t} * g(|\mathbf{r} - \mathbf{r}'|, t) \right]$$

$$+ [\mathbf{E}(\mathbf{r}', t) \cdot \mathbf{n}] * \nabla' g(|\mathbf{r} - \mathbf{r}'|, t) \} + 0.5 \mathbf{E}(\mathbf{r}, t) \tag{20}$$

In fact, here the integral over S is denoted in terms of Cauchy principle value and singular point's contribution. We rewrite (20) as

$$\int_{-\infty}^{t} c^2 \nabla \nabla \cdot \mathbf{A}(\mathbf{r}, \tau) d\tau - \partial_t \mathbf{A}(\mathbf{r}, t) - \varepsilon^{-1} \nabla \times \mathbf{F}(\mathbf{r}, t)$$

$$= 0.5 \mathbf{E}(\mathbf{r}, t) + \int_{-\infty}^{t} c^2 \nabla \nabla \cdot \underline{\mathbf{A}}(\mathbf{r}, \tau) d\tau - \partial_t \underline{\mathbf{A}}(\mathbf{r}, t) - \varepsilon^{-1} \nabla \times \underline{\mathbf{F}}(\mathbf{r}, t) \tag{21}$$

In the above equation, $\underline{\mathbf{A}}$ and $\underline{\mathbf{F}}$ denote the integrals (7) and (8) with the singular point removed from them. Similarly, we may have

$$\int_{-\infty}^{t} c^2 \nabla \nabla \cdot \mathbf{F}(\mathbf{r}, \tau) d\tau - \partial_t \mathbf{F}(\mathbf{r}, t) + \mu^{-1} \nabla \times \mathbf{A}(\mathbf{r}, t)$$

$$= 0.5 \mathbf{H}(\mathbf{r}, t) + \int_{-\infty}^{t} c^2 \nabla \nabla \cdot \underline{\mathbf{F}}(\mathbf{r}, \tau) d\tau - \partial_t \underline{\mathbf{F}}(\mathbf{r}, t) + \mu^{-1} \nabla \times \underline{\mathbf{A}}(\mathbf{r}, t) \tag{22}$$

Actually, the computation of $v_i^m(t)$ is performed in terms of

elements, and we will encounter integrals given by

$$I_{e0}^{mn} = \iint_{S^m} \mathbf{t}_i^m(\mathbf{r}) \cdot [\partial_t \mathbf{E}^i(\mathbf{r}, t) + 0.5 \partial_t \mathbf{E}(\mathbf{r}, t)] dS \tag{23}$$

$$I_{h0}^{mn} = \iint_{S^m} \mathbf{S}_i^m(\mathbf{r}) \cdot [\partial_t \mathbf{H}^i(\mathbf{r}, t) + 0.5 \partial_t \mathbf{H}(\mathbf{r}, t)] dS \tag{24}$$

$$I_{e1}^{mn} = \iint_{S^m} \mathbf{t}_i^m(\mathbf{r}) \cdot \iint_{S^n} g(|\mathbf{r} - \mathbf{r}'|, t) * \mathbf{J}(\mathbf{r}', t) dS' dS \tag{25}$$

$$I_{h1}^{mn} = \iint_{S^m} \mathbf{S}_i^m(\mathbf{r}) \cdot \iint_{S^n} g(|\mathbf{r} - \mathbf{r}'|, t) * \mathbf{M}(\mathbf{r}', t) dS' dS \tag{26}$$

$$I_{e2}^{mn} = \iint_{S^m} \mathbf{t}_i^m(\mathbf{r}) \cdot \iint_{S^n} \nabla g(|\mathbf{r} - \mathbf{r}'|, t) * \times \mathbf{M}(\mathbf{r}', t) dS' dS \tag{27}$$

$$I_{h2}^{mn} = \iint_{S^m} \mathbf{S}_i^m(\mathbf{r}) \cdot \iint_{S^n} \nabla g(|\mathbf{r} - \mathbf{r}'|, t) * \times \mathbf{J}(\mathbf{r}', t) dS' dS \tag{28}$$

$$I_{e3}^{mn} = \iint_{S^m} \mathbf{t}_i^m(\mathbf{r}) \cdot \nabla \iint_{S^n} g(|\mathbf{r} - \mathbf{r}'|, t) * \nabla_s' \cdot \mathbf{J}(\mathbf{r}', t) dS' dS \tag{29}$$

$$I_{h3}^{mn} = \iint_{S^m} \mathbf{S}_i^m(\mathbf{r}) \cdot \nabla \iint_{S^n} g(|\mathbf{r} - \mathbf{r}'|, t) * \nabla_s' \cdot \mathbf{M}(\mathbf{r}', t) dS' dS \tag{30}$$

where $\mathbf{S}_i^m = \mathbf{n} \times \mathbf{W}_i^m$ and $\mathbf{t}_i^m = \mathbf{n} \times \mathbf{n} \times \mathbf{W}_i^m$. On obtaining (29) and (30), we have used (16) and (17).

Let us examine the above integrals. Obviously, I_{e0}^{mn} and I_{h0}^{mn} are regular integrals. As source point $\mathbf{r}'$ close to field point $\mathbf{r}$, I_{e1}^{mn} and I_{h1}^{mn} are of $1/R$ singularity, which may be calculated numerically. However, I_{e2}^{mn}, I_{h2}^{mn}, I_{e3}^{mn} and I_{h3}^{mn} are of $1/R^2$ singularity. Thus, it is difficult to calculate them accurately by numerical method, and further measures have to be taken to reduce their singularity.

Fortunately, examining (27) and (28) carefully, we may find that I_{e2}^{mn} and I_{h2}^{mn} vanish if S^m and S^n are on the same plane. As for I_{e3}^{mn} and I_{h3}^{mn}, applying Gauss divergence theorem to them, we may get

$$I_{e3}^{mn} = \int_{\partial S^m} \mathbf{t}_i^m(\mathbf{r}) \cdot \mathbf{n}_c \left[\iint_{S^n} g(|\mathbf{r} - \mathbf{r}'|, t) * \nabla_s' \cdot \mathbf{J}(\mathbf{r}', t) dS' \right] d\Gamma \tag{31}$$

and

$$I_{h3}^{mn} = \iint_{S^m} \nabla_s \cdot \mathbf{S}_i^m(\mathbf{r}) \left[\iint_{S^n} g(|\mathbf{r} - \mathbf{r}'|, t) * \nabla_s' \cdot \mathbf{M}(\mathbf{r}', t) dS' \right] dS \tag{32}$$

where ∂S^m denotes the boundary of S^m, and n_c is the outward unit vector normal to ∂S^m, lying in the plane of S^m. So, I_{e3}^{mn} and I_{h3}^{mn} are also of $1/R$ singularity as $\mathbf{r}'$ close to $\mathbf{r}$.

Up to now, it seems that $v_i^m(t)$ may be calculated conveniently by numerical method. However, here, a problem is with (31). With (10) and (11), it may be shown that $\nabla'_s \cdot \mathbf{J}(\mathbf{r}', t) = 0$, which will lead to a completely wrong result for I_{e3}^{mn}. This problem can be accounted for by the numerical errors introduced by the way of obtaining the electric current $\mathbf{J}$. For, the Whitney 1-form basis functions used in (11) are of "linear" functions (Actually, they are of order 0.5), consequently, within each element, the electric current $\mathbf{J}$ obtained by (10) is a constant, and hence, its divergence is zero.

Here, we will present our remedy for this problem. According to the definition of surface divergence, we may have

$$\nabla'_s \cdot \mathbf{J}(\mathbf{r}', t) = -\partial_t [\varepsilon_0 \mathbf{E}(\mathbf{r}', t) \cdot \mathbf{n}] \tag{33}$$

By using the above identity, I_{e3}^{mn} is written as

$$I_{e3}^{mn} = -\int_{\partial S^m} \mathbf{t}_i^m(\mathbf{r}) \cdot \mathbf{n}_c \left\{ \iint_{S^n} g(|\mathbf{r}-\mathbf{r}'|, t) * \partial_t [\varepsilon_0 \mathbf{E}(\mathbf{r}', t) \cdot \mathbf{n}] dS' \right\} d\Gamma \tag{34}$$

which can avoid the above problem.

In fact, this problem hasn't been encountered in other integral equation methods, such as time domain integral equation (TDIE) method, or even in frequency domain FE-BI method. Essentially, it can be attributed to the routine of the time domain FE-BI method, where either electric field or magnetic field is taken as the variable, and the other field is obtained by numerical method. For example, here, electric field is taken as the variable, and the tangential component of magnetic field (i.e., equivalent electric current) on boundary S is obtained by (10). This problem can be circumvented by the remedy presented here.

After the above treatments, and with the contribution of singular point has been computed analytically, $v_i^m(t)$ can be calculated by numerical method e.g., by Gaussian quadrature. And applying a traditional central difference scheme to (12) yields

$$\boldsymbol{A}e^{n+1} = (2\boldsymbol{T} - \Delta t^2 \boldsymbol{S})e^n + [0.5\Delta t(\boldsymbol{R} + \boldsymbol{Q}) - \boldsymbol{T}]e^{n-1} - \Delta t^2 v^n \tag{35}$$

where $e^n = e(n\Delta t)$, $v^n = v(n\Delta t)$, and $\boldsymbol{A} = \boldsymbol{T} + 0.5\Delta t(\boldsymbol{R} + \boldsymbol{Q})$.

It is worthy of being pointed out here that by adopting the central difference scheme, the required electric and magnetic currents on the surface S for the computation of column vector v^n at each time step are known quantities, and so the sparseness and symmetry of finite element matrices are well preserved. Namely, while it reduces

the computational domain, the proposed scheme using one auxiliary boundary will not contaminate the finite element matrices.

Apparently, to update electric field with (35), we have to solve a matrix equation at each time step. However, matrix $\boldsymbol{A}$ is time-invariant, and is highly sparse. Hence, the matrix equation can be solved efficiently. Generally, a direct solver is suitable for small- and medium-sized problems, and matrix $\boldsymbol{A}$ has to be factorized only once. Whereas an iterative solver is more attractive for large-scale problems, and the preconditioner also has to be constructed only once.

4. NUMERICAL RESULTS

This section presents numerical examples to demonstrate the validity and performance of the proposed scheme. We first examine the accuracy of proposed scheme with respect to that of previous one, and that of the frequency domain FE-BI method. Then we will give an analysis of the CPU time and memory requirements with the proposed scheme compared to the previous one as direct solver is considered for Equation (35).

For the examples considered herein, we use a Neumann pulse as excitation

$$\mathbf{E}^i(\mathbf{r}, t) = \mathbf{E}_0[t - t_0 - c^{-1}\hat{\mathbf{k}} \cdot (\mathbf{r} - \mathbf{r}_0)] \exp\left\{-[t - t_0 - c^{-1}\hat{\mathbf{k}} \cdot (\mathbf{r} - \mathbf{r}_0)]^2/\tau^2\right\} \tag{36}$$

where $\hat{\mathbf{k}}$ and $\mathbf{E}_0$ denote the direction of propagation and polarization of the incident pulse, respectively, and t_0, r_0, and τ are parameters that define the pulse's temporal and spectral reference points and width.

The radar cross section (RCS) is computed as

$$\sigma = \lim_{r \to \infty} 4\pi r^2 \frac{|F[\mathbf{E}^{far}(\mathbf{r}, t)]|^2}{|F[\mathbf{E}^i(\mathbf{r}, t)]|^2} \tag{37}$$

where $F[\cdot]$ denotes Fourier transform, and $\mathbf{E}^{far}(\mathbf{r}, t)$ represents the scattered electric field in the far-field zone, which is evaluated by

$$r\mathbf{E}^{far}(\mathbf{r}, t + c^{-1}r) = (4\pi c)^{-1}\partial_t \iint_S [\hat{\mathbf{r}} \times \mathbf{M}(\mathbf{r}', t + c^{-1}\hat{\mathbf{r}} \cdot \mathbf{r}')$$
$$+ \eta_0 \hat{\mathbf{r}} \times \hat{\mathbf{r}} \times \mathbf{J}(\mathbf{r}', t + c^{-1}\hat{\mathbf{r}} \cdot \mathbf{r}')]dS' \tag{38}$$

where η_0 is the free space intrinsic impedance, $r = |\mathbf{r}|$, and $\hat{\mathbf{r}} = \frac{\mathbf{r}}{r}$.

4.1. Accuracy

We first examine the accuracy of the proposed scheme with respect to that of the previous one by considering the scattering problem of a conducting sphere. And next, the accuracy of the proposed scheme is also compared with that of the frequency domain FE-BI method as the scattering from a coated sphere is analyzed.

A. Conducting sphere. The radius of the PEC sphere is 0.1 m. The pulse parameters are $\mathbf{E}_0 = \hat{\mathbf{x}}$, $\hat{\mathbf{k}} = \hat{\mathbf{z}}$, $\tau = 5.25$ ns, $t_0 = 15$ ns, and $\mathbf{r}_0 = -1.2\mathrm{m}\,\hat{\mathbf{z}}$. For the proposed scheme, the truncation boundary (also as the source boundary) is a spherical surface positioned a single element away from the PEC surface. The computational domain is discretized with tetrahedra, yielding 242 edges with 72 edges on the truncation boundary. As for the scheme using two auxiliary boundaries, the source boundary is placed one element away from the PEC surface, and the truncation boundary is in turn placed one element away from the source boundary. For comparison, same discretization has been adopted on the truncation boundary as the above one, yielding 412 edges (also with 72 edges on truncation boundary for this case). Equation (35) is solved by direct method, and the time step is $\Delta t = 25$ ps.

The bistatic RCS and frequency response of static RCS obtained from the two schemes are given by Fig. 2 and Fig. 3, respectively, where scheme A denotes the proposed scheme and scheme B denotes the scheme that uses two auxiliary boundaries. It may be seen that the results obtained from the two schemes both agree well with exact solutions, almost having the same accuracy.

We note that, beyond the range approximately from 40 MHz to 250 MHz, the computed results become worse as the frequency becomes higher or lower, as shown in Fig. 3. This can be accounted for by the pulse's spectrum, whose amplitude decays seriously as the frequency is too high or too low. For example, when $f = 250$ MHz, the pulse's spectrum decays to 4.29×10^{-7} times its peak value. To achieve accurate results for higher frequency, we have to broaden the width of the pulse's spectrum by reducing its parameter τ, and in the meantime, a finer discretization is required, correspondingly.

B. Coated sphere. As stated earlier, in the sense of one auxiliary boundary being used, the proposed scheme may be viewed as the extension of the frequency domain FE-BI method to the time domain. By considering the scattering problem of a coated sphere, we would like to show its accuracy with respect to that of its frequency counterpart, too. The radii of the coated sphere and the conducting core are 0.13 m and 0.1 m, respectively. The dielectric layer has a relative permittivity $\varepsilon_r = 2$, and a relative permeability $\mu_r = 1$. The pulse parameters are
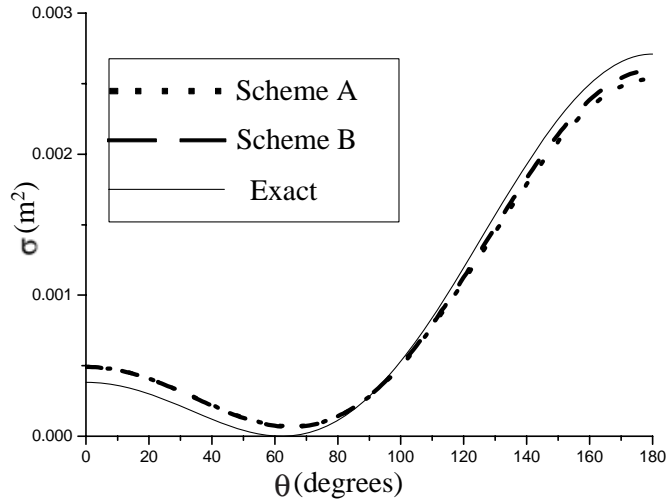
Figure 2. E-plane bistatic RCS of a conducting sphere (f = 150 MHz).
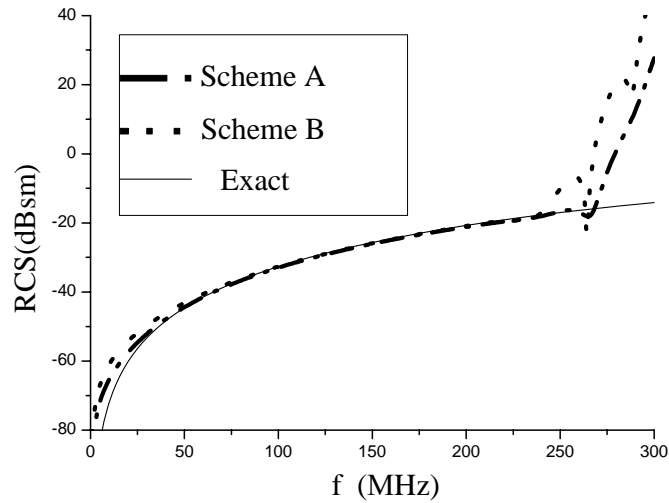

Figure 3. Backscatter RCS versus frequency of a conducting sphere.

identical to those of the above case. We directly choose the coated spherical surface as the truncation boundary. The discretization of computational region yields 242 edges. The time step is $\Delta t = 25$ ps. The backscattered temporal electric field obtained by the proposed

scheme is given in Fig. 4 ($rE_Z = 0$, and this can be explained by (38)). To compare with the solutions gained by the frequency domain FE-BI method, the temporal result is converted into frequency domain RCS shown in Fig. 5. As demonstrated in Fig. 5, the results from the two methods accord each other well. Incidentally, the results obtained for the frequencies beyond the width of the pulse's spectrum by the time domain FE-BI method are inaccurate as well, and they have not been presented here.
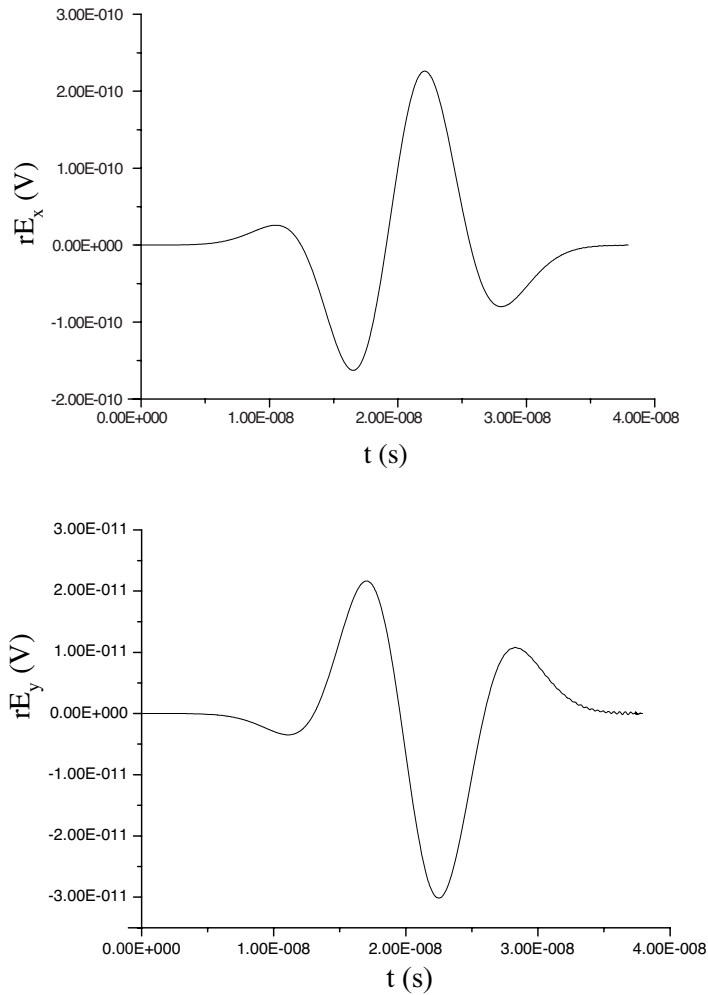
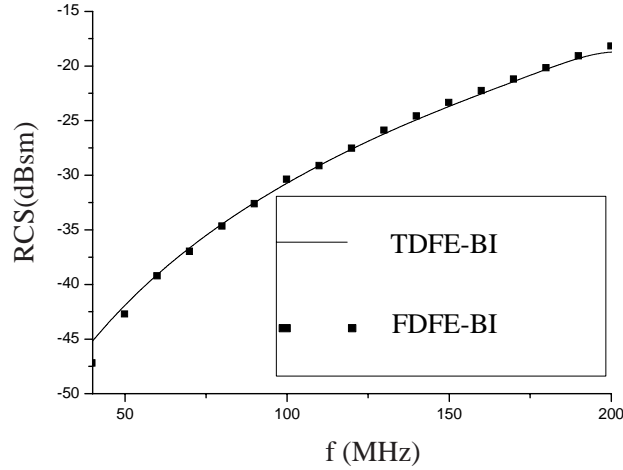**Figure 4.** Backscattered far-field response of a coated sphere in time domain.

Figure 5. Comparison of frequency response of static RCS obtained by frequency- and time-domain methods.

4.2. Computational costs

Here we perform the analysis of the computational costs for the two schemes by considering, as an example, scattering from a coated sphere, where the conducting core is with different given radii. The pulse parameters, the thick of dielectric layer and its relative permittivity are assumed to be the same as those of example B considered above. The computational region is divided into tetrahedra.

For the proposed scheme, the dielectric surface is chosen as the truncation boundary, and a one-element layer has been set between the truncation boundary and the PEC surface. For the scheme using two auxiliary boundaries, the dielectric surface is used as source boundary, and a one-element layer has been set between the source boundary and the PEC surface. However, for this case, an additional layer of elements has to be adopted outside the source boundary. So, a two-layer element has been placed between the truncation boundary and the PEC surface for this scheme. For comparison, we have adopted same discretization on the truncation boundaries for the two schemes, where the edges' length is about 0.1 m.

We consider applying a direct sparse matrix solver to Equation (35), and matrix $\boldsymbol{A}$ is factorized by LDL^T method. Because matrix $\boldsymbol{A}$ is time-invariant, the factorization is performed only once. Sparse memory storage technique is used for the matrices in Equation (35). As R (the radius of the conducting core) is with different given val-
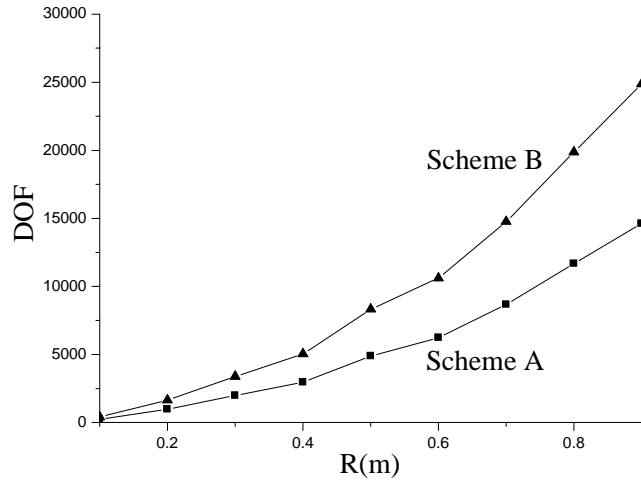
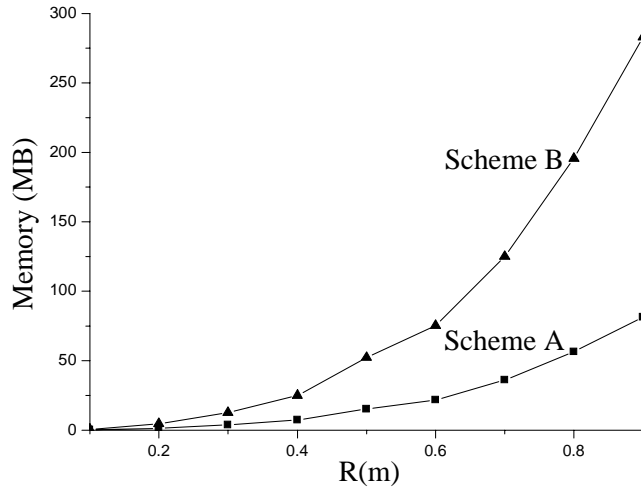**Figure 6.** Degrees of freedom with the two schemes.

Figure 7. Required memory with the two schemes.

ues, the overall degrees of freedom, required memory, and CPU time consumed by the factorization for the two schemes are presented in Fig. 6, Fig. 7, and Fig. 8, respectively. We may see that, compared to the previous one, the proposed scheme reduces the overall degrees of freedom, which in turn decreases the required memory and CPU time significantly, especially as the radius being larger, as demonstrated in Fig. 7 and Fig. 8.
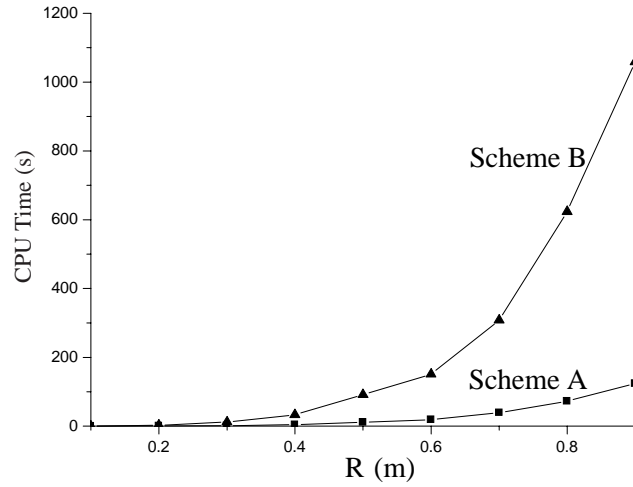
Qiu et al.

Figure 8. CPU time with the two schemes.

5. CONCLUSION

This paper has proposed an improved time domain FE-BI scheme for 3-D scattering. Contrary to the scheme reported in the literature, the proposed scheme uses only one auxiliary boundary, serving both as truncation and source boundary, by which the computational domain for finite elements has been reduced. And in the meantime, the sparseness and symmetry of the finite element matrices have been well preserved. So it is a more efficient scheme for the time domain FE-BI method. The treatment of the singularity of Green's function with this scheme has been addressed in detail. Finally, the accuracy and efficiency of the proposed scheme were verified by numerical examples.

REFERENCES

1. Paulsen, K. D., D. R. Lynch, and J. W. Strobehn, "Three-dimensional finite, boundary, and hybrid element solutions of Maxwell equations for lossy dielectric media," *IEEE Trans. Microwave Theory Tech.*, Vol. 36, 682–693, Apr. 1988.
2. Shen, X. Q., J. M. Jin, J. Song, C. C. Lu, and W. C. Chew, "On the formulation of hybrid finite-element and boundary-integral methods for 3-D scattering," *IEEE Trans. Antennas Propagat.*, Vol. 46, 303–311, Mar. 1998.
3. Liu, J. and J. M. Jin, "A novel hybridization of higher order

finite element and boundary integral methods for electromagnetic scattering and radiation problems," *IEEE Trans. Antennas Propagat.*, Vol. 49, 1794–1806, Dec. 2001.

4. Botha, M. M. and J. M. Jin, "Adaptive finite element-boundary integral analysis for electromagnetic fields in 3-D," *IEEE Trans. Antennas Propagat.*, Vol. 53, 1710–1720, May 2005.

5. Zhang, Y. J. and E. P. Li, "Scattering of three-dimensional chiral objects above a perfect conducting plane by hybrid finite element method," *J. Electromagn. Waves Appl.*, Vol. 19, 1535–1546, 2005.

6. Qiu, Z. J., X. Y. Hou, X. Li, and J. D. Xu, "On the condition number of matrices from various hybrid vector FEM-BEM formulations for 3-D scattering," *J. Electromagn. Waves Appl.*, Vol. 20, 1797–1806, 2006.

7. Gao, S., L. W. Li, and A. Sambell, "FETD analysis of a dual-frequency microstrip patch antenna," *Progress In Electromagnetics Research*, PIER 54, 155–178, 2005.

8. Gong, Z. and G. Q. Zhu, "FDTD analysis of an anisotriopically coated missile," *Progress In Electromagnetics Research*, PIER 64, 69–80, 2006.

9. Pingenot, J., R. N. Rieben, D. A. White, and D. G. Dudley, "Full wave analysis of RF signal attenuation in a rough surface cave using a higher order time domain vector finite element method," *J. Electromagn. Waves Appl.*, Vol. 20, 1695–1705, 2006.

10. Jiao, D., M. Lu, E. Michielssen, and J. M. Jin, "A fast time-domain finite element-boundary integral method for electromagnetic analysis," *IEEE Trans. Antennas Propagat.*, Vol. 49, 1453–1461, Oct. 2001.

11. McCowen, A., A. J. Radcliffe, and M. S. Towers, "Time-domain modeling of scattering from arbitrary cylinders in two dimensions using a hybrid finite-element and integral equation method," *IEEE Trans. Magn.*, Vol. 39, 1227–1229, May 2003.

12. Jiao, D., A. A. Ergin, B. Shanker, E.Michielssen, and J. M. Jin, "A fast higher-order time-domain finite element-boundary integral method for 3-D electromagnetic scattering analysis," *IEEE Trans. Antennas Propagat.*, Vol. 50, 1192–1202, Sep. 2002.

13. Rao, S. M. and D. R. Wilton, "E-field, H-field, and combined field solution for arbitrarily shaped three-dimensional dielectric bodies," *Electromagn.*, Vol. 10, 407–421, 1990.

14. Bossavit, A., "Whitney forms: a class of finite elements for three-dimensional computation in electromagnetism," *IEE Proc.*, Vol. 135, 493–500, Nov. 1988.